Supplementary Information

High-throughput automated droplet microfluidic system for screening of reaction conditions.

Krzysztof Churski, Piotr Korczyk, Piotr Garstecki*

Received (in XXX, XXX) Xth XXXXXXXXX 200X, Accepted Xth XXXXXXXXX 200X
First published on the web Xth XXXXXXXXX 200X
DOI: 10.1039/b000000x

Videos

- **dropletHTS_352x242px_operation_of_the_system_25fps_real_time.avi**, The video presents an exemplary sequence of droplets and shows merging of packs of three droplets of native solutions into the 'reaction' droplets. Played back at the same rate at which it was recorded.
- **dropletHTS_64x104px_scan_of_concentrations_15fps_real_time.avi**,
The video shows droplets forming a sequence that scans the all combinations of concentrations of two inks. This video (at a larger resolution) was used to extract the data presented in Figure 3a. Played back at the same rate at which it was recorded.

Construction of the valve and connections

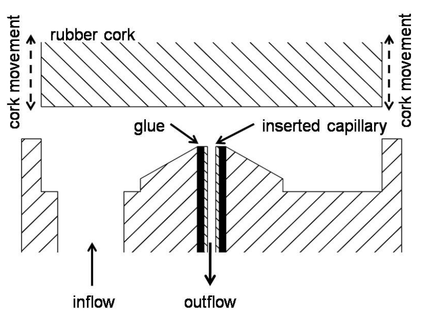

Fig. 1 The scheme shows the cross-section of the capillary valve. Into the standard outflow from the chamber of electromagnetic valve we inserted a steel capillary (I.D. 205 μm, O.D. 400 μm) and filled the space between the capillary and the body of the valve with the glue. The valve is closed when the rubber cork is in a 'down' position and blocks outflow from chamber. When it is up, the valve is open and fluid flows out. The modified valve presents an ~10^4 higher resistance to outflow than to inflow. This feature allows for dispensing of small quantities of fluid and avoids pushing out the liquid upon closer of the rubber plunger.

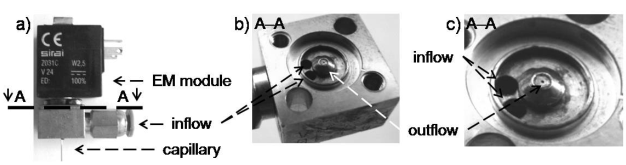

Fig. 2. The photographs show the electromagnetic valve with the resistive capillary and the chamber of the valve.

Image analysis.

The videos of sequences of droplets were recorded with a high-speed color camera (Photron 1024C). These videos were analyzed with a custom written script in Matlab. This script automatically recogniezed droplets and numbered them in the sequence. The frames showing droplest were used to retrive the avarage RGB signal from the interior of the droplet. Than each of the intensities I_R, I_G and I_B (adopting values between 0 and 255) were divided by the intensities I_{R0}, I_{G0} and I_{B0} of the background.

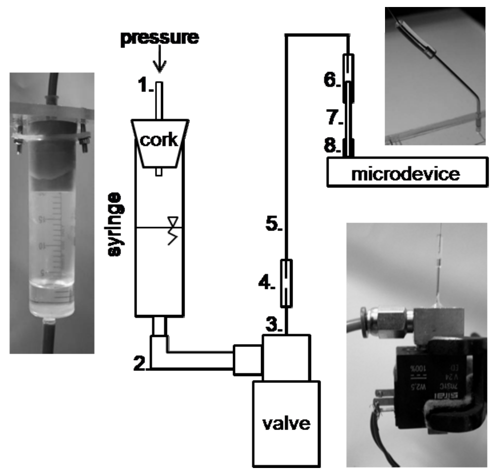

Fig. 3. The scheme presents connections of elements of our system. The flow of liquid is driven by a pressure applied to a container (a syringe). The pressure is exerted by compressed air via a pressure reduction valve. The large diameter pneumatic tubing is interfaced with the reservior via a steel needle ((1) I.D. 0.7 mm, O.D. 0.9 mm). The syringe is connected to the valve via a large diameter tubing ((2) I.D. 2 mm, O.D. 4 mm). Fluid flows out from the valve through a steel capillaries ((3) I.D. 0.2 mm, O.D. 1.1 mm) and ((5) I.D. 0.2 mm, O.D. 0.4 mm). Capillaries (3) and (5) are connected wth a short section of the Tygoon® tubing ((4) I.D. 0.25 mm, O.D. 2.07 mm) . A similar section (6) connects the capillary (5) and a steel capillary ((7) I.D. 0.6 mm, O.D. 0.8 mm). Finally, a section of poliethylene tubing PE60 ((8) I.D. 0.76 mm, O.D. 1.22 mm) interfaces the steel capillary with the hole (I.D. 1.2 mm) in a polycarbonate or polydimethylosiloxane chip.

We than calculated the signals S_R, S_G and S_B as $S = - \ln (I/I_0)$. These singals should be—via the Lambert-Beer law—proportional to the concentration of the ink (with different coefficients of proportionality for each of the inks). We first used solutions of known concentrations of each of the inks to form droplets, record their images and retrive the calibration curves S([ink]). We found that these curves diverged slightly from linear relations – probably due to reflection of light at the menisci of the droplets. We fitted the calibration curves with polynomials of order 3 and than used these polynomials in the analysis of the screens of concentrations of the two inks (data presented in Figure 3 in the manuscript).